

Adversarial Training: Enhancing Out-of-Distribution Generalization for Learning Wireless Resource Allocation

Shengjie Liu and Chenyang Yang

Abstract—Deep neural networks (DNNs) have widespread applications for optimizing resource allocation. Yet, their performance is vulnerable to distribution shifts between training and test data, say channels. In this letter, we resort to adversarial training (AT) for enhancing out-of-distribution (OOD) generalizability of DNNs trained in unsupervised manner. We reformulate AT to capture the OOD degradation, and propose a one-step gradient ascent method for AT. The proposed method is validated by optimizing hybrid precoding. Simulation results showcase the enhanced OOD performance of multiple kinds of DNNs across various channel distributions, when only Rayleigh fading channels are used for training.

Index Terms—Out-of-distribution generalization, adversarial training, unsupervised learning, hybrid precoding.

I. INTRODUCTION

DEEP learning is widely used for optimizing resource allocation in wireless systems, by designing deep neural networks (DNNs) to learn the mapping from environment parameters (say channels) into optimized resources [1]. With closed-form expressions of objective function and constraints, DNNs can be trained in unsupervised manner, hence the computations for generating labels are avoided [1], [2].

Majority of existing works assume that training and test data are identically distributed. When the DNNs are tested on data with unseen distributions, their out-of-distribution (OOD) performance often degrades obviously. In wireless communications, the distribution of environment parameters, especially channels, may vary rapidly due to many factors such as the changed locations of users and scatterers [3]. Although DNNs can be fine-tuned online with transfer learning, meta-learning, *etc.*, collecting and training with new datasets are time-consuming. Limited by the up-to-date data and computing resources, such adaptations are infeasible in highly dynamic wireless environments [3] where the channel statistics change in tens of seconds [4]. Hence, improving the OOD generalizability of DNNs is crucial for their practical use.

Only a few research efforts attempt to increase the OOD generalization performance of deep learning for wireless applications. A data generation method was proposed in [5], which however requires the knowledge of possible channel distributions for testing. A hyper-network was designed in [6] to generate weights for a deep unfolding network, thereby enhancing its OOD performance. It was reported in [7] that deep unfolding itself exhibits acceptable performance on unseen distributions. Nonetheless, deep unfolding needs task-specific design, which restricts their applicability.

To achieve good OOD performance, distributionally robust optimization (DRO) [8] was introduced. In order to be well-generalized across a range of distributions, DRO optimizes

the weights of a DNN for performing better on the worst-case distribution. Unfortunately, DRO is hard to be solved [8].

Adversarial training (AT) can be regarded as an easy-to-implement alternative to DRO [9], [10]. AT was originally proposed to defend against adversarial attacks. Specifically, AT algorithms, exemplified by [11], generate adversarial examples (i.e., the misleading samples with crafted perturbations) and adjust the weights of DNNs with these examples.

Both DRO and AT have been investigated only in the context of supervised learning, and can not be applied to unsupervised learning. Defense for adversarial attacks has also been studied in supervised learning-based wireless solutions [12]. However, the viability of using AT to enhance OOD generalization remains unexplored in wireless communications.

In this letter, we resort to AT for improving the OOD generalizability of the DNNs that are trained unsupervisedly for optimizing resource allocation. The major contributions are summarized as follows. (1) To find the worst-case distribution in unsupervised learning, we reformulate DRO and AT, enabling them to be aware of the deterioration of DNNs. (2) We propose a method, namely unsupervised AT (UAT), to solve the reformulated AT problem. (3) We evaluate the OOD performance gain from the UAT on diverse channel distributions by training several DNNs only on Rayleigh channels, for optimizing hybrid precoding that maximizes sum-rate (SR) under quality of service (QoS) constraints.

II. PRELIMINARY

We first recap the DRO and AT in supervised learning.

Denote \mathbf{x} as the input and \mathbf{y}^* as the label for supervised learning, where the pair $(\mathbf{x}, \mathbf{y}^*)$ follows a given distribution \mathcal{D} during training. A DNN $f_{\mathbf{y}}(\mathbf{x}; \boldsymbol{\theta})$ parameterized by $\boldsymbol{\theta}$ can produce an output \mathbf{y} . The accuracy of the output can be improved by optimizing $\boldsymbol{\theta}$ with a loss function $L(\mathbf{y}, \mathbf{y}^*)$.

To obtain satisfactory OOD performance on unknown distributions, DRO, minimizing the expected loss on the worst-case distribution $\hat{\mathcal{D}}$ that incurs the highest loss, is formulated as [8]

$$\min_{\boldsymbol{\theta}} \max_{\mathcal{D}' \in \mathbb{D}} \mathbb{E}_{(\mathbf{x}, \mathbf{y}^*) \sim \mathcal{D}'} [L(f_{\mathbf{y}}(\mathbf{x}; \boldsymbol{\theta}), \mathbf{y}^*)], \quad (1)$$

where $\mathbb{D} = \{\mathcal{D}' | W(\mathcal{D}', \mathcal{D}) \leq \varepsilon\}$ is the set of distributions around \mathcal{D} , $W(\cdot, \cdot)$ denotes the Wasserstein distance between two distributions, and ε is a threshold.

Although solving (1) enables the DNN to achieve minimal loss over all distributions in \mathbb{D} , the impossibility of sampling from the unsolved $\hat{\mathcal{D}}$ renders the problem intractable [8].

To defend against adversarial attacks, AT is formulated as follows to minimize the expected loss over the most “maliciously” perturbed inputs $\tilde{\mathbf{x}}$ [11],

$$\min_{\boldsymbol{\theta}} \mathbb{E}_{(\mathbf{x}, \mathbf{y}^*) \sim \mathcal{D}} \left[\max_{\tilde{\mathbf{x}} \in B_{\varepsilon}(\mathbf{x})} L(f_{\mathbf{y}}(\tilde{\mathbf{x}}; \boldsymbol{\theta}), \mathbf{y}^*) \right], \quad (2)$$

The authors are with Beihang University, Beijing 100191, China (e-mail: liushengjie, cyyang@buaa.edu.cn).

where $B_\epsilon(\mathbf{x}) = \{\mathbf{x} + \boldsymbol{\delta} \mid \|\boldsymbol{\delta}\|_2 \leq \epsilon\}$ is the set of allowed perturbations around \mathbf{x} , and ϵ is the perturbation range.

Differing from (1), the ‘‘optimization variable’’ in (2), $\tilde{\mathbf{x}}$, is a sample rather than a distribution, which is referred to as the *adversarial example* of \mathbf{x} . Since the expectation in (2) can be approximated by averaging over samples drawn from \mathcal{D} , this problem can be solved by alternately executing the following two steps [11]: (i) **Find** $\tilde{\mathbf{x}}$: It can be obtained using gradient ascent methods, guided by the partial derivative of loss function with respect to (w.r.t.) \mathbf{x} . (ii) **Update** $\boldsymbol{\theta}$: It can be optimized using back-propagation, with the loss averaged over all adversarial examples.

Previous studies have proved that the objective in (1) is upper bounded by the objective in (2) asymptotically (say Corollary 2 in [9], Theorems 1 and 2 in [10]). Consequently, DNNs trained by AT algorithms can also exhibit favorable OOD generalizability [10]. However, existing works never investigate DRO or AT for unsupervised deep learning.

III. ADVERSARIAL TRAINING IN UNSUPERVISED LEARNING

In this section, we formulate DRO and AT for unsupervised learning, and propose a method for solving the AT problem.

A. Problem Reformulation

With environment parameter \mathbf{x} , resource allocation can be optimized from the following problem

$$\min_{\mathbf{y}} F(\mathbf{x}, \mathbf{y}) \quad \text{s.t. } G_i(\mathbf{x}, \mathbf{y}) \leq 0, i = 1, \dots, N_C. \quad (3)$$

The optimal solutions for every value of \mathbf{x} constitute a function $\mathbf{y}^* = f_{\mathbf{y}^*}(\mathbf{x})$. When a DNN $\mathbf{y} = f_{\mathbf{y}}(\mathbf{x}; \boldsymbol{\theta})$ is trained to learn this function, \mathbf{x} follows a distribution \mathcal{D} .

Unsupervised *primal-dual learning* (PDL) [1], [2] can be adopted to train the DNN, which can be formulated as

$$\max_{\boldsymbol{\xi}} \min_{\boldsymbol{\theta}} \mathbb{E}_{\mathbf{x} \sim \mathcal{D}} [\mathcal{L}(\mathbf{x}; \boldsymbol{\theta}, \boldsymbol{\xi})], \quad (4)$$

where $\mathcal{L}(\mathbf{x}; \boldsymbol{\theta}, \boldsymbol{\xi})$ is a Lagrangian function defined as follows

$$\mathcal{L}(\mathbf{x}; \boldsymbol{\theta}, \boldsymbol{\xi}) = F(\mathbf{x}, f_{\mathbf{y}}(\mathbf{x}; \boldsymbol{\theta})) + \sum_{i=1}^{N_C} f_{\lambda_i}(\mathbf{x}; \boldsymbol{\xi}) G_i(\mathbf{x}, f_{\mathbf{y}}(\mathbf{x}; \boldsymbol{\theta})), \quad (5)$$

and $f_{\lambda_i}(\mathbf{x}; \boldsymbol{\xi})$ is the i th element of an *multiplier network* $f_{\lambda}(\mathbf{x}; \boldsymbol{\xi})$ [2].

To improve OOD performance, we consider DRO with a cost $F(\mathbf{x}, \mathbf{y})$,¹ which determines the worst-case distribution.

Analogous to (1), one can optimize the weights of DNNs on the distribution $\tilde{\mathcal{D}}$ with the highest cost, i.e., $\max_{\tilde{\mathcal{D}} \in \mathbb{D}} \mathbb{E}_{\mathbf{x} \sim \tilde{\mathcal{D}}} [F(\mathbf{x}, f_{\mathbf{y}}(\mathbf{x}; \boldsymbol{\theta}))]$. However, $\tilde{\mathcal{D}}$ obtained in this way is NOT the worst-case distribution, because this objective cannot differentiate the cost increase caused by the *higher optimal objective value* and by the *degraded generalization performance* of $f_{\mathbf{y}}(\cdot; \boldsymbol{\theta})$ on the distributions in \mathbb{D} . The former is unrelated to generalizability. For example, for SR-maximization resource allocation, a decrease in channel strength inevitably increases the cost (i.e., reduces SR), but a DNN may not perform worse on low-strength channels.

¹‘‘Cost’’ is a metric of interest. If one seeks to further guarantee the constraints on unseen distributions, $F(\mathbf{x}, \mathbf{y}) + \sum_{i=1}^{N_C} \max(0, G_i(\mathbf{x}, \mathbf{y}))$ can be used as the cost, and the subsequent analysis is similar.

Optimizing the DNN on such channels may not be beneficial for OOD generalization.

To address this issue,² we reformulate DRO as

$$P_{\text{DRO}} : \max_{\boldsymbol{\xi}} \min_{\boldsymbol{\theta}} \mathbb{E}_{\mathbf{x} \sim \tilde{\mathcal{D}}} [\mathcal{L}(\mathbf{x}; \boldsymbol{\theta}, \boldsymbol{\xi})] \quad (6a)$$

$$\text{s.t. } \tilde{\mathcal{D}} = \arg \max_{\tilde{\mathcal{D}} \in \mathbb{D}} \mathbb{E}_{\mathbf{x} \sim \tilde{\mathcal{D}}} [F(\mathbf{x}, f_{\mathbf{y}}(\mathbf{x}; \boldsymbol{\theta})) - F(\mathbf{x}, f_{\mathbf{y}^*}(\mathbf{x}))], \quad (6b)$$

for training $f_{\mathbf{y}}(\cdot; \boldsymbol{\theta})$ and $f_{\lambda}(\cdot; \boldsymbol{\xi})$ on the *true worst-case distribution*, where the DNN $f_{\mathbf{y}}(\cdot; \boldsymbol{\theta})$ has the largest gap in cost from the optimal solution instead of the highest cost.

Inspired by [10], we adopt AT as a realizable alternative to the DRO for enhancing OOD generalizability performance. By replacing $\tilde{\mathcal{D}}$ by $\tilde{\mathbf{x}}$, the AT problem for unsupervised PDL is formulated as

$$P_{\text{AT}} : \max_{\boldsymbol{\xi}} \min_{\boldsymbol{\theta}} \mathbb{E}_{\mathbf{x} \sim \mathcal{D}} [\mathcal{L}(\tilde{\mathbf{x}}; \boldsymbol{\theta}, \boldsymbol{\xi})] \quad (7a)$$

$$\text{s.t. } \tilde{\mathbf{x}} = \arg \max_{\mathbf{x}' \in B_\epsilon(\mathbf{x})} [F(\mathbf{x}', f_{\mathbf{y}}(\mathbf{x}'; \boldsymbol{\theta})) - F(\mathbf{x}', f_{\mathbf{y}^*}(\mathbf{x}'))]. \quad (7b)$$

B. Unsupervised Adversarial Training (UAT) Method

To solve P_{AT} , we first find the adversarial example $\tilde{\mathbf{x}}$ for every original sample \mathbf{x} from (7b).

Recall the definitions of $\tilde{\mathbf{x}} = \mathbf{x} + \boldsymbol{\delta}$ and $B_\epsilon(\mathbf{x})$ in (2), (7b) can be transformed into a problem to optimize $\boldsymbol{\delta}$ as follows

$$\max_{\|\boldsymbol{\delta}\|_2 \leq \epsilon} F(\mathbf{x} + \boldsymbol{\delta}, f_{\mathbf{y}}(\mathbf{x} + \boldsymbol{\delta}; \boldsymbol{\theta})) - F(\mathbf{x} + \boldsymbol{\delta}, f_{\mathbf{y}^*}(\mathbf{x} + \boldsymbol{\delta})). \quad (8)$$

To find $\boldsymbol{\delta}$ (and hence find $\tilde{\mathbf{x}}$) with low complexity, we employ one-step gradient ascent method. By using the first-order Taylor polynomial, it can be seen that (8) has the same solution as the following problem when ϵ is very small,

$$\max_{\|\boldsymbol{\delta}\|_2 \leq \epsilon} \left(\frac{\partial F(\mathbf{x}, f_{\mathbf{y}}(\mathbf{x}; \boldsymbol{\theta}))}{\partial \mathbf{x}} - \frac{dF(\mathbf{x}, f_{\mathbf{y}^*}(\mathbf{x}))}{d\mathbf{x}} \right)^T \boldsymbol{\delta}. \quad (9)$$

It is not hard to show that the optimal solution of (9) is

$$\boldsymbol{\delta} = \epsilon \cdot \frac{\frac{\partial F(\mathbf{x}, f_{\mathbf{y}}(\mathbf{x}; \boldsymbol{\theta}))}{\partial \mathbf{x}} - \frac{dF(\mathbf{x}, f_{\mathbf{y}^*}(\mathbf{x}))}{d\mathbf{x}}}{\left\| \frac{\partial F(\mathbf{x}, f_{\mathbf{y}}(\mathbf{x}; \boldsymbol{\theta}))}{\partial \mathbf{x}} - \frac{dF(\mathbf{x}, f_{\mathbf{y}^*}(\mathbf{x}))}{d\mathbf{x}} \right\|_2}. \quad (10)$$

To obtain the value of $\frac{\partial F(\mathbf{x}, f_{\mathbf{y}}(\mathbf{x}; \boldsymbol{\theta}))}{\partial \mathbf{x}} - \frac{dF(\mathbf{x}, f_{\mathbf{y}^*}(\mathbf{x}))}{d\mathbf{x}}$, we rewrite its first term by using the chain rule as

$$\frac{\partial F(\mathbf{x}, f_{\mathbf{y}}(\mathbf{x}; \boldsymbol{\theta}))}{\partial \mathbf{x}} = \frac{\partial F}{\partial \mathbf{x}} + \frac{\partial F}{\partial \mathbf{y}} \cdot \frac{\partial f_{\mathbf{y}}(\mathbf{x}; \boldsymbol{\theta})}{\partial \mathbf{x}}, \quad (11)$$

where the values of partial derivatives $\frac{\partial F}{\partial \mathbf{x}}$ and $\frac{\partial F}{\partial \mathbf{y}}$ are computed with the value of \mathbf{y} produced by $f_{\mathbf{y}}(\mathbf{x}; \boldsymbol{\theta})$, and $\frac{\partial f_{\mathbf{y}}(\mathbf{x}; \boldsymbol{\theta})}{\partial \mathbf{x}}$ can be obtained from the DNN due to its differentiability.

Obtaining the value of the second term is challenging owing to the unknown function $f_{\mathbf{y}^*}(\cdot)$. To cope with this difficulty, we invoke the *envelope theorem* [13]. Then, the gradient of the optimal objective can be obtained directly from (3) as

$$\frac{dF(\mathbf{x}, f_{\mathbf{y}^*}(\mathbf{x}))}{d\mathbf{x}} = \frac{\partial F}{\partial \mathbf{x}} + \lambda_1^*(\mathbf{x}) \frac{\partial G_1}{\partial \mathbf{x}} + \dots + \lambda_{N_C}^*(\mathbf{x}) \frac{\partial G_{N_C}}{\partial \mathbf{x}}, \quad (12)$$

where $\lambda_1^*(\mathbf{x}), \dots, \lambda_{N_C}^*(\mathbf{x})$ are the optimal Lagrange multipliers for the N_C constraints in (3), which depend on \mathbf{x} .

²This issue does not arise in supervised learning, where the cost is the same as the loss function, because the optimal cost/loss is always zero.

Unlike (11), the values of partial derivatives in (12) are computed with the value of optimal solution \mathbf{y}^* . In practice, the value of \mathbf{y}^* can be approximated by the output of $\mathbf{y} = f_{\mathbf{y}}(\mathbf{x}; \boldsymbol{\theta})$, since \mathbf{x} herein is an in-distribution (ID) sample and $f_{\mathbf{y}}(\cdot; \boldsymbol{\theta})$ has been trained with all ID samples before UAT begins. Similarly, the values of $\lambda_1^*(\mathbf{x}), \dots, \lambda_{N_C}^*(\mathbf{x})$ can be approximated by the outputs of multiplier network $f_{\lambda}(\mathbf{x}; \boldsymbol{\xi})$.

By combining (11) and (12), we have

$$\frac{\partial F(\mathbf{x}, f_{\mathbf{y}}(\mathbf{x}; \boldsymbol{\theta}))}{\partial \mathbf{x}} - \frac{dF(\mathbf{x}, f_{\mathbf{y}^*}(\mathbf{x}))}{d\mathbf{x}} = \frac{\partial F}{\partial \mathbf{y}} \cdot \frac{\partial f_{\mathbf{y}}}{\partial \mathbf{x}} - \sum_{i=1}^{N_C} f_{\lambda_i} \frac{\partial G_i}{\partial \mathbf{x}}. \quad (13)$$

By substituting (13) into (10), the adversarial example of \mathbf{x} , i.e., $\tilde{\mathbf{x}} = \mathbf{x} + \boldsymbol{\delta}$, can be obtained as

$$\tilde{\mathbf{x}} = \mathbf{x} + \epsilon \cdot \left\| \frac{\partial F}{\partial \mathbf{y}} \cdot \frac{\partial f_{\mathbf{y}}(\mathbf{x}; \boldsymbol{\theta})}{\partial \mathbf{x}} - \sum_{i=1}^{N_C} f_{\lambda_i}(\mathbf{x}; \boldsymbol{\xi}) \frac{\partial G_i}{\partial \mathbf{x}} \right\|_2 \triangleq \mathbf{x} + \epsilon \cdot d(\mathbf{x}). \quad (14)$$

With a batch of adversarial examples, (7a) can be optimized by standard back-propagation algorithms (say Adam algorithm), where $\mathcal{L}(\cdot; \boldsymbol{\theta}, \boldsymbol{\xi})$ is computed using the adversarial examples rather than the original samples.

To solve P_{AT} , the optimizations in (7b) and (7a) are alternately executed for T iterations. In the first iteration, the adversarial examples are generated from the original samples using (14). In the subsequent iterations, the adversarial examples are generated from those obtained in the previous iteration. In this way, the range of perturbations can be expanded for facilitating OOD generalization, meanwhile in each iteration ϵ can be set as a small value for the Taylor approximation being accurate.

Remark 1: The constraints in (3) for some wireless problems are imposed on \mathbf{y} but not related to \mathbf{x} . For instance, power constraint is independent of channels. Such constraints can be ensured via projection methods, and render the multiplier network $f_{\lambda}(\mathbf{x}; \boldsymbol{\xi})$ unnecessary. For these problems, $\frac{\partial G_i}{\partial \mathbf{x}} = 0$ in (12). By contrast, for the problems with complex constraints (say the QoS constraints) that are related to \mathbf{x} (say channels), $f_{\lambda}(\mathbf{x}; \boldsymbol{\xi})$ is required and the values of corresponding partial derivatives $\frac{\partial G_i}{\partial \mathbf{x}}$ in (12) ought to be computed.

The proposed method is summarized in Algorithm 1, where Lines 8~15 are the steps specifically for UAT and other lines are for PDL. The lines marked with an asterisk (*) can be omitted if there are no constraints related to \mathbf{x} .

Remark 2: The training complexity of UAT is T times higher than PDL. As a training method, UAT does not affect the inference complexity of DNNs.

IV. CASE STUDY: OPTIMIZING HYBRID PRECODING

In this section, we apply UAT for optimizing QoS-constrained hybrid precoding.

Consider a base station (BS) equipped with N_T antennas and N_{RF} radio frequency (RF) chains, which serves K single-antenna users. The analog and baseband precoders can be jointly optimized to maximize SR as follows [14],

$$\max_{\mathbf{W}_{RF}, \mathbf{W}_{BB}} \sum_{k=1}^K R_k \quad (15a)$$

$$\text{s.t. } \|\mathbf{W}_{RF} \mathbf{W}_{BB}\|_F^2 = P_{\text{tot}}, \quad (15b)$$

$$|(\mathbf{W}_{RF})_{n,j}| = 1, n = 1, \dots, N_T, j = 1, \dots, N_{RF}, \quad (15c)$$

$$R_k \geq \gamma_k, k = 1, \dots, K, \quad (15d)$$

Algorithm 1 Unsupervised Adversarial Training (UAT)

Input: number of epochs E , number of batches B , batch-size N_B , samples $\{\mathbf{x}_n\}_{n=1}^{BN_B}$, initial weight $\boldsymbol{\theta}$, learning rate η_1, η_2 , epoch to begin UAT E_A , number of adversarial iterations T , perturbation range ϵ
 * initialized weight of multiplier network $\boldsymbol{\xi}$

- 1: **for** $epoch = 1, \dots, E$ **do**
- 2: **for** $batch = 1, \dots, B$ **do**
- 3: $\mathcal{N} = \{1 + N_B(batch - 1), \dots, N_B(batch)\}$
- 4: $\mathcal{L} = \frac{1}{N_B} \sum_{n \in \mathcal{N}} F(\mathbf{x}_n, f_{\mathbf{y}}(\mathbf{x}_n; \boldsymbol{\theta}))$
- 5: * $\mathcal{L} \leftarrow \mathcal{L} + \frac{1}{N_B} \sum_{n \in \mathcal{N}} \sum_{i=1}^{N_C} f_{\lambda_i}(\mathbf{x}_n; \boldsymbol{\xi}) G_i(\mathbf{x}_n, f_{\mathbf{y}}(\mathbf{x}_n; \boldsymbol{\theta}))$
- 6: $\boldsymbol{\theta} \leftarrow \boldsymbol{\theta} - \eta_1 \frac{\partial \mathcal{L}}{\partial \boldsymbol{\theta}}$
- 7: * $\boldsymbol{\xi} \leftarrow \boldsymbol{\xi} + \eta_2 \frac{\partial \mathcal{L}}{\partial \boldsymbol{\xi}}$
- 8: **if** $epoch \geq E_A$ **then** ▷ UAT begins
- 9: $\tilde{\mathbf{x}}_n^0 = \mathbf{x}_n, \forall n \in \mathcal{N}$
- 10: **for** $t = 1, \dots, T$ **do**
- 11: $\tilde{\mathbf{x}}_n^t = \tilde{\mathbf{x}}_n^{t-1} + \epsilon \cdot d(\tilde{\mathbf{x}}_n^{t-1}), \forall n \in \mathcal{N}$ ▷ see (14)
- 12: $\mathcal{L} = \frac{1}{N_B} \sum_{n \in \mathcal{N}} F(\tilde{\mathbf{x}}_n^t, f_{\mathbf{y}}(\tilde{\mathbf{x}}_n^t; \boldsymbol{\theta}))$
- 13: * $\mathcal{L} \leftarrow \mathcal{L} + \frac{1}{N_B} \sum_{n \in \mathcal{N}} \sum_{i=1}^{N_C} f_{\lambda_i}(\tilde{\mathbf{x}}_n^t; \boldsymbol{\xi}) G_i(\tilde{\mathbf{x}}_n^t, f_{\mathbf{y}}(\tilde{\mathbf{x}}_n^t; \boldsymbol{\theta}))$
- 14: $\boldsymbol{\theta} \leftarrow \boldsymbol{\theta} - \eta_1 \frac{\partial \mathcal{L}}{\partial \boldsymbol{\theta}}$ ▷ via back-propagation
- 15: * $\boldsymbol{\xi} \leftarrow \boldsymbol{\xi} + \eta_2 \frac{\partial \mathcal{L}}{\partial \boldsymbol{\xi}}$ ▷ via back-propagation

Output: trained weight $\boldsymbol{\theta}$

where $R_k = \log_2 \left(1 + \frac{|\mathbf{h}_k^H \mathbf{W}_{RF} \mathbf{W}_{BB} \mathbf{e}_k|^2}{\sum_{i=1, i \neq k}^K |\mathbf{h}_i^H \mathbf{W}_{RF} \mathbf{W}_{BB} \mathbf{e}_k|^2 + \sigma^2} \right)$, $\mathbf{h}_k \in \mathbb{C}^{N_T}$, and γ_k are the achievable rate, channel vector, and data-rate requirement of the k th user, respectively, $\mathbf{W}_{RF} \in \mathbb{C}^{N_T \times N_{RF}}$ is the analog precoder, $\mathbf{W}_{BB} = [\mathbf{w}_{BB1}, \dots, \mathbf{w}_{BBK}] \in \mathbb{C}^{N_{RF} \times K}$ is the baseband precoder, P_{tot} is the total power, and σ^2 is the noise power. (15b) is the power constraint, (15c) is the constant modulus constraint for the analog precoder, and (15d) is the QoS constraint for every user.

In this task, $\mathbf{H} = [\mathbf{h}_1, \dots, \mathbf{h}_K]^T \in \mathbb{C}^{K \times N_T}$ is the environment parameter. To adapt to a wide range of transmit power and channel strength, $\text{SNR} \triangleq \|\mathbf{H}\|_F^2 P_{\text{tot}} / \sigma^2$ is also regarded as an environment parameter. Then, the DNN for learning the hybrid precoding is $(\mathbf{W}_{RF}, \mathbf{W}_{BB}) = f_{\mathbf{y}}(\mathbf{H} / \|\mathbf{H}\|_F, \text{SNR}; \boldsymbol{\theta})$ with two inputs, where the channel is normalized to avoid redundancy in the input information. Meanwhile, since both (15b) and (15c) are unrelated to \mathbf{H} and can be guaranteed by the projection method in [15], only the K QoS constraints in (15d) need to be satisfied using a multiplier network denoted as $f_{\lambda}(\mathbf{H} / \|\mathbf{H}\|_F, \text{SNR}; \boldsymbol{\xi})$.

When applying UAT, we only need to generate adversarial examples for $\mathbf{H} / \|\mathbf{H}\|_F$, since SNR is a scalar with finite range that does not need to be generalized. To ensure that the adversarial examples are normalized, we modify (14) as

$$\tilde{\mathbf{x}} = \frac{\mathbf{x} + \epsilon \cdot d(\mathbf{x})}{\|\mathbf{x} + \epsilon \cdot d(\mathbf{x})\|_2}. \quad (16)$$

V. SIMULATION RESULTS

In this section, we evaluate the OOD performance of DNNs trained by the proposed UAT for the hybrid precoding task.

We use the following two metrics to evaluate performance. Average SR (ASR) is the averaged SR over a test set, where the SR of a sample is recorded as zero if the constraints are

not satisfied. Violation Ratio (VR) is the proportion of samples in a test set that violate the constraints.

To obtain a benchmark for comparison, we simulate a difference-of-convex (DC) programming-based numerical algorithm [14] to optimize hybrid precoders. Instead of selecting from the array responses computed by the angles of departure (AoDs) of all propagation paths [14], we set \mathbf{W}_{RF} as the phases of the first N_{RF} right singular vectors of \mathbf{H} .

In simulations, the BS equipped with $N_T = 16$ antennas and $N_{RF} = 6$ RF chains serves $K = 4$ users with data-rate requirements of $\gamma_1 = \dots = \gamma_K = 1$ bps/Hz. P_{tot}/σ^2 is uniformly selected from the range of 0~20 dB during training, and is set as 10 dB for testing unless otherwise specified.

We compare UAT with two existing AT methods in [10], [11]. They are also incorporated into PDL but generate adversarial examples in other ways. Following the configurations in [10], [11], the number of descent steps is 7, step size is 2, and projection radius is 8. For UAT, the tuned hyper-parameters are $E_A = 50$, $T = 5$, $\epsilon = 5$. The PDL in [2] without any AT serves as a baseline.

Both $f_y(\cdot; \theta)$ and $f_\lambda(\cdot; \xi)$ are realized by three kinds of DNNs designed for hybrid precoding: convolutional neural networks (CNN) [16], three-dimensional graph neural network (3D-GNN) [15], and recursive GNN (RGNN) [17]. The optimizer is Adam, $\eta_1 = \eta_2 = 0.001$, $N_B = 100$, batch normalization is used for CNN and 3D-GNN, activation function is $\text{Tanh}(\cdot)$ for RGNN and $\text{ReLU}(\cdot)$ for CNN and 3D-GNN. Other hyper-parameters are listed in Table I, where 3×3 convolution kernels are used in the hidden layers of CNN followed by a fully-connected layer with 512 neurons.

TABLE I
FINE-TUNED HYPER-PARAMETERS

Kind of DNN	$f_y(\cdot; \theta)$		$f_\lambda(\cdot; \xi)$	
	Number of hidden layers	Number of channels in layers	Number of hidden layers	Number of channels in layers
CNN	5	[256, ..., 256, 16]	3	[128, 128, 16]
3D-GNN	6	[256, ..., 256]	4	[128, ..., 128]
RGNN	4	[64, 64, 64, 16]	3	[32, 32, 8]

These DNNs are trained with 100,000 samples of Rayleigh fading channel (i.e., $\mathbf{h}_k \sim \mathcal{CN}(\mathbf{0}, \mathbf{I}_{N_T})$). Once trained, they are not fine-tuned, in order for examining their OOD generalization performance.

The performances of the DNNs trained with different methods are evaluated on several test sets, each consisting of 2,000 samples generated from unseen channel distributions (referred to as OOD test samples), as detailed in the sequel.

A. Rician Fading Channel

The OOD test samples are generated from the following Rician fading channel model

$$\mathbf{h}_k = \sqrt{\kappa/(\kappa+1)}\mathbf{a}(\phi_k) + \sqrt{1/(\kappa+1)}\mathbf{z}_k, \quad (17)$$

where $\mathbf{a}(\phi_k) = [1, e^{i\pi \sin(\phi_k)}, \dots, e^{i(N_T-1)\pi \sin(\phi_k)}]^T$ is the array response of the line-of-sight (LOS) path with AoD $\phi_k \sim \mathcal{U}(0, 2\pi)$, $\mathbf{z}_k \sim \mathcal{CN}(\mathbf{0}, \mathbf{I}_{N_T})$, and κ is the Rician factor.

In Fig. 1, we provide the performance of training RGNN by PDL or UAT, with legend PDL(ID) or UAT(ID) when tested in Rayleigh channel and legend PDL(OOD) or UAT(OOD) when tested in Rician channel. Fig. 1(a) shows that RGNN

trained by both methods can achieve comparable ASR to DC in Rayleigh channel. When tested in Rician channel, the RGNN trained by UAT attains a 4.7% higher ASR (normalized by DC) than the RGNN trained by PDL. Fig. 1(b) shows that DC can satisfy QoS constraints for all samples on both channels. When tested in Rayleigh channel, RGNN trained by both methods exhibits extremely low VR (about 0.3%). When tested in Rician channels, the RGNN trained by UAT has a 4.9% lower VR than that trained by PDL, thanks to the consistent objective in (15a) and constraints in (15d), even though no constraint satisfaction is considered in the cost of our DRO formulation. Besides, the inference time of RGNN is 15.48 ms, but DC requires 5498 ms on the same CPU.

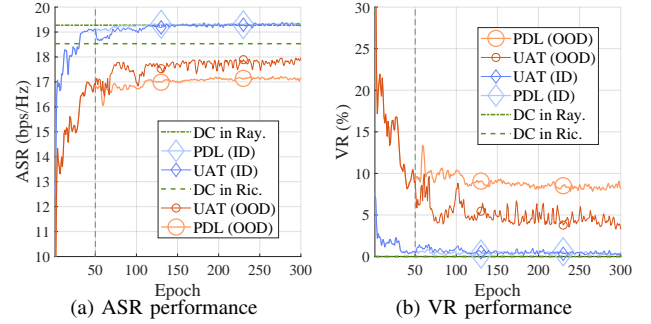


Fig. 1. Performance of RGNN on ID test samples (Rayleigh) and OOD test samples (Rician, $\kappa = 10$ dB), during training with PDL or UAT.

In Fig. 2, we compare the OOD generalization performance of RGNN and 3D-GNN trained by different methods. When the distribution of test samples differs noticeably from Rayleigh channel (say $\kappa \geq 10$ dB), UAT improves OOD generalization by approximately 5% in both ASR and VR for the two GNNs. The ASR of UAT-trained DNNs still retains 85% of the ASR of DC even when $\kappa = 20$ dB. The DNNs trained by the AT methods in [10], [11] exhibit marginal OOD generalization gains over PDL, due to not designed for unsupervised learning. Their performance degradation observed at $\kappa \leq 5$ dB (close to Rayleigh channels, i.e., ID samples) results from their overly broad perturbation range.

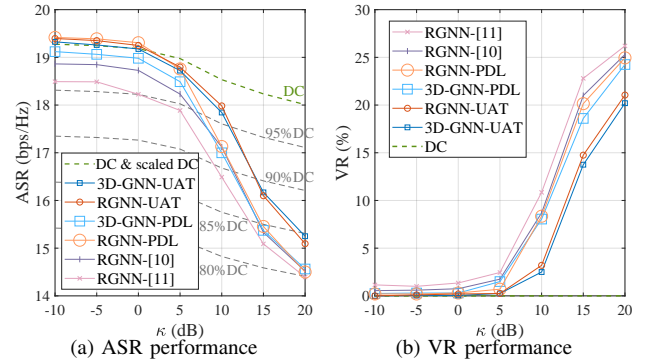


Fig. 2. OOD performance of two GNNs trained with different methods.

B. Spatially Correlated Channel

The OOD test samples are generated from the following spatially correlated channel model [18]

$$\mathbf{H} = \mathbf{R}_U^{\frac{1}{2}} \mathbf{Z} \mathbf{R}_A^{\frac{1}{2}}, \quad (18)$$

where each element in \mathbf{Z} is $z_{k,n} \sim \mathcal{CN}(0, 1)$, $\mathbf{R}_A \in \mathbb{R}^{N_T \times N_T}$ is the antenna correlation matrix with element in the i th row

and j th column being $\rho_A^{|i-j|}$, $\mathbf{R}_U \in \mathbb{R}^{K \times K}$ captures the inter-user correlation with diagonal elements being 1 and off-diagonal elements being ρ_U , and $\rho_A, \rho_U \in [0, 1]$.

In Table II, we provide the OOD generalization performance of the DNNs trained by PDL or UAT when they are tested on correlated channels. As shown by the values in boldface, the OOD generalization gains of UAT over PDL are more pronounced in highly correlated channels ($\rho_U, \rho_A \geq 0.6$), which often arise in scenarios with densely distributed users, limited scatters, or closely spaced antennas. In particular, for RGNN, the OOD gain ranges from 4.1% (i.e., 99.7%–95.6%, shown in red) to 20.3% (shown in green, similarly hereafter), whereas for 3D-GNN, the gain ranges from 3.1% to 13.8%. The lower gain of 3D-GNN is attributed to its inherent relatively better OOD generalizability. For CNN, UAT significantly boosts ASR by 10.2%~22.6% across all values of ρ_U and ρ_A , not limited to highly correlated channels. This is because UAT can mitigate the overfitting of CNN.

TABLE II
ASR PERFORMANCE (RELATIVE TO DC) IN CORRELATED CHANNELS

		ρ_U varies ($\rho_A = 0$)				ρ_A varies ($\rho_U = 0$)			
		0.2	0.4	0.6	0.8	0.2	0.4	0.6	0.8
DC (bps/Hz)		18.77	17.62	15.65	12.36	19.13	18.86	18.14	16.26
RGNN	PDL	100.3%	99.2%	91.3%	72.6%	100.6%	99.1%	95.6%	78.3%
	UAT	99.9%	98.8%	95.8%	87.4%	100.4%	100.3%	99.7%	98.6%
3D-GNN	PDL	98.7%	97.3%	93.8%	79.2%	99.1%	98.5%	96.4%	84.9%
	UAT	100.0%	99.4%	98.1%	93.0%	100.3%	99.9%	99.5%	95.5%
CNN	PDL	82.2%	80.0%	74.2%	57.6%	82.6%	81.9%	80.2%	70.5%
	UAT	92.5%	91.3%	89.2%	80.2%	92.8%	92.1%	91.3%	84.0%

C. Sparse Channel and 3GPP Channel

Finally, the OOD test samples are generated from two millimeter-wave channel models, which are commonly used for hybrid precoding. The first is an L -path sparse channel,

$$\mathbf{h}_k = \sqrt{N_T/L} \sum_{l=1}^L \alpha_{k,l} \mathbf{a}(\phi_{k,l}), \quad (19)$$

where $\alpha_{k,l} \sim \mathcal{CN}(0, 1)$ is a complex gain, and $\mathbf{a}(\phi_{k,l})$ is the array response for AoD $\phi_{k,l} \sim \mathcal{U}(0, 2\pi)$.

The second is a more realistic channel model specified in 3GPP TR 38.901 [19], with a carrier frequency of 28 GHz.³

In Table III, we provide the OOD generalization performance of the DNNs trained by PDL or UAT when they are tested on the two kinds of channels. It is evident that UAT enhances the OOD generalizability of all three DNNs, even for the LOS and NLOS scenarios in 3GPP channel model. The results in boldface indicate that 3D-GNN outperforms both RGNN and CNN in terms of OOD generalization.

VI. CONCLUSIONS

In this letter, we reformulated AT for unsupervisedly training OOD-generalizable DNNs to optimize wireless resource allocation. We proposed the UAT method to solve the formulated AT problem, and applied the method to train three different DNNs for learning QoS-aware hybrid precoding. Simulation results showed that these DNNs trained by the

³ P_{tot} is 49 dBm for UMa and 44 dBm for UMi scenarios. In LOS scenarios, P_{tot} is further reduced by 20 dB to avoid the extra high received power that results in nonlinear distortion. σ^2 is -85 dBm. Owing to the difference in large-scale fading channels among users, QoS constraints are hard to be satisfied and thus are omitted.

TABLE III
ASR PERFORMANCE (RELATIVE TO DC) IN SPARSE & 3GPP CHANNELS

		Sparse Channels				Scenarios in TR 38.901			
		Number of paths, L				UMa	UMa	UMi	UMi
		5	4	3	2	NLOS	LOS	NLOS	LOS
DC (bps/Hz)		18.28	18.24	17.93	17.43	9.74	15.44	14.89	16.84
RGNN	PDL	96.6%	95.0%	89.7%	80.2%	95.0%	88.1%	73.8%	82.6%
	UAT	97.8%	96.1%	92.7%	84.6%	111.3%	100.5%	91.7%	96.1%
3D-GNN	PDL	96.4%	95.7%	93.1%	86.0%	97.0%	91.5%	76.4%	87.2%
	UAT	99.1%	98.4%	96.6%	90.2%	117.2%	103.9%	95.1%	100.3%
CNN	PDL	77.4%	75.8%	70.5%	60.8%	95.9%	77.8%	69.4%	74.2%
	UAT	87.9%	86.0%	80.8%	70.3%	102.6%	86.2%	77.3%	82.7%

proposed method can achieve superior OOD generalization on Rician fading, spatially correlated, sparse, and 3GPP channels, by being trained only on Rayleigh fading channels.

REFERENCES

- [1] M. Eisen, C. Zhang, L. F. O. Chamon, D. D. Lee, and A. Ribeiro, "Learning optimal resource allocations in wireless systems," *IEEE Trans. Signal Process.*, vol. 67, no. 10, pp. 2775–2790, May 2019.
- [2] C. Sun and C. Yang, "Learning to optimize with unsupervised learning: Training deep neural networks for URLLC," *IEEE PIMRC*, 2019.
- [3] M. Akrouf, A. Feriani, F. Bellili, A. Mezghani, and E. Hossain, "Domain generalization in machine learning models for wireless communications: Concepts, state-of-the-art, and open issues," *IEEE Commun. Surv. Tutor.*, vol. 25, no. 4, pp. 3014–3037, 2023.
- [4] K. Haneda, J. Zhang, L. Tan *et al.*, "5G 3GPP-like channel models for outdoor urban microcellular and macrocellular environments," *IEEE VTC Spring*, 2016.
- [5] D. Luan and J. Thompson, "Achieving robust generalization for wireless channel estimation neural networks by designed training data," *IEEE ICC*, 2023.
- [6] J. Zhang, C.-K. Wen, and S. Jin, "Adaptive MIMO detector based on hypernetwork: Design, simulation, and experimental test," *IEEE J. Sel. Areas Commun.*, vol. 40, no. 1, pp. 65–81, Jan. 2022.
- [7] X. He, L. Huang, J. Wang, and Y. Gong, "Learn to optimize RIS aided hybrid beamforming with out-of-distribution generalization," *IEEE Trans. Veh. Technol.*, vol. 73, no. 7, pp. 10783–10787, Jul. 2024.
- [8] J. Liu, Z. Shen, Y. He, X. Zhang, R. Xu, H. Yu, and P. Cui, "Towards out-of-distribution generalization: A survey," *arXiv:2108.13624*, 2021.
- [9] R. Gao and A. Kleywegt, "Distributionally robust stochastic optimization with wasserstein distance," *Mathematics of Operations Research*, vol. 48, no. 2, pp. 603–655, 2023.
- [10] M. Yi, L. Hou, J. Sun, L. Shang, X. Jiang, Q. Liu, and Z. Ma, "Improved OOD generalization via adversarial training and pre-training," *ICML*, 2021.
- [11] A. Madry, A. Makelov, L. Schmidt, D. Tsipras, and A. Vladu, "Towards deep learning models resistant to adversarial attacks," *ICLR*, 2018.
- [12] D. Adesina, C.-C. Hsieh, Y. E. Sagduyu, and L. Qian, "Adversarial machine learning in wireless communications using RF data: A review," *IEEE Commun. Surv. Tutor.*, vol. 25, no. 1, pp. 77–100, 2023.
- [13] A. Takayama, *Mathematical economics*. Cambridge university press, 1985.
- [14] G. Niu, Q. Cao, and M.-O. Pun, "QoS-aware resource allocation for mobile edge networks: User association, precoding and power allocation," *IEEE Trans. Veh. Technol.*, vol. 70, no. 12, pp. 12617–12630, Dec. 2021.
- [15] S. Liu, J. Guo, and C. Yang, "Multidimensional graph neural networks for wireless communications," *IEEE Trans. Wireless Commun.*, vol. 23, no. 4, pp. 3057–3073, Apr. 2024.
- [16] A. M. Elbir, K. V. Mishra, M. R. B. Shankar, and B. Ottersten, "A family of deep learning architectures for channel estimation and hybrid beamforming in multi-carrier mm-Wave massive MIMO," *IEEE Trans. Cogn. Commun. Netw.*, vol. 8, no. 2, pp. 642–656, Jun. 2022.
- [17] J. Guo and C. Yang, "Recursive GNNs for learning precoding policies with size-generalizability," *IEEE Trans. Mach. Learn. Commun. Netw.*, vol. 2, pp. 1558–1579, 2024.
- [18] X. Wu and D. Liu, "Novel insight into multi-user channels with multi-antenna users," *IEEE Commun. Lett.*, vol. 21, no. 9, pp. 1961–1964, Sep. 2017.
- [19] 3GPP, "Study on channel model for frequencies from 0.5 to 100 GHz," TR 38.901, Version 17.0.0, Mar. 2022.